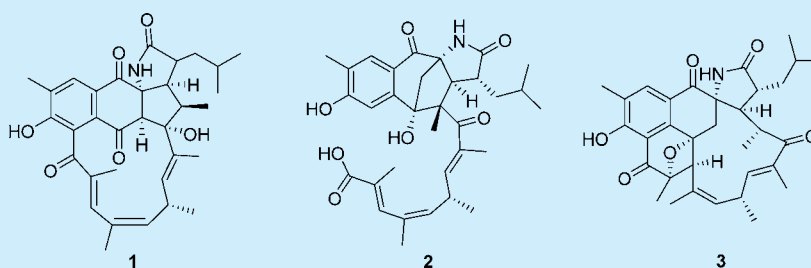


## Ansalactams B–D Illustrate Further Biosynthetic Plasticity within the Ansamycin Pathway

Tu Cam Le,<sup>†,§</sup> Inho Yang,<sup>†,§</sup> Yeo Joon Yoon,<sup>†</sup> Sang-Jip Nam,<sup>\*,†</sup> and William Fenical<sup>\*,‡</sup><sup>†</sup>Department of Chemistry and Nano Science, Global Top 5 program, Ewha Womans University, Seoul 03760, Korea<sup>‡</sup>Center for Marine Biotechnology and Biomedicine, Scripps Institution of Oceanography, University of California San Diego, La Jolla, California 92093-0204, United States

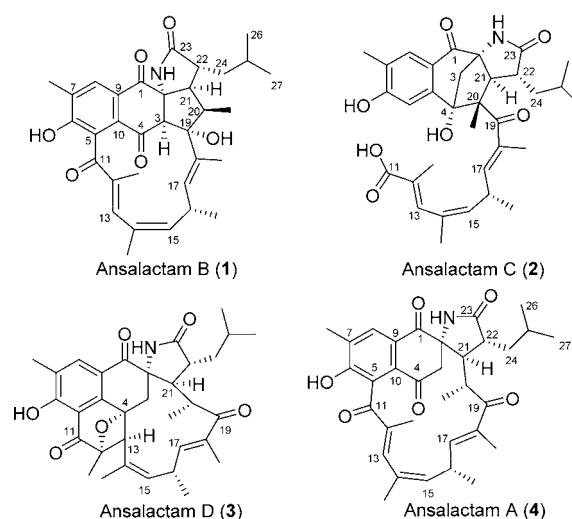
## S Supporting Information



**ABSTRACT:** Further chemical investigation of a marine-derived bacterium of the genus *Streptomyces* has led to the isolation of ansalactams B–D (1–3) along with the previously reported metabolite ansalactam A (4). Ansalactams B–D are significantly modified ansamycins, representing three new carbon skeletons and further illustrating the biosynthetic plasticity of the ansalactam class. Unlike ansalactam A, ansalactams B and D are penta- and hexacyclic metabolites, while ansalactam C illustrates an open polyene chain with a terminal carboxylic acid.

The ansamycin class of polyketides such as rifamycin SV, ansamitosin P-3, and geldanamycin represents some of the most potent microbially produced antibiotics and anticancer agents.<sup>1,2</sup> These drugs are produced by bacteria of the order Actinomycetales, the most prolific source of structurally diverse metabolites of all known microorganisms.<sup>3</sup> Over the past 15 years, we have focused our efforts on actinomycetes from underexplored marine environments such as deep oceans, marine sediments, and marine surfaces. Chemical investigations of microbes from these environments have led to the isolation of structurally unique secondary metabolites with diverse biological activities.<sup>4,5</sup> Recently, our streptomycete strain CNH189 was found to produce two structurally unrelated natural products, ansalactam A,<sup>6</sup> an ansamycin polyketide, and the merochlorins,<sup>7</sup> meroterpenoid antibiotics derived from an unusual hybrid polyketide–terpenoid biosynthetic pathway. Based upon the diverse biosynthetic capacity of this strain, we carefully examined this strain and report here three new ansamycin analogues, ansalactams B–D (1–3), each of which is composed of a unique, undescribed carbon skeleton. As with ansalactam A, these new derivatives also incorporate the 4-methyl-2-pentenoic acid polyketide extender unit, forming the  $\gamma$ -lactam ring. In this paper, we describe the isolation and structure elucidation of ansalactams B–D (1–3), their suggested biosynthetic origins, and their biological activities.

The molecular formula of ansalactam B (1) was assigned as  $C_{33}H_{39}NO_6$  on the basis of the analysis of HRESIMS data (a protonated molecular ion peak at  $m/z$  546.2850  $[M + H]^+$ ) and



on interpretation of  $^{13}C$  NMR data. Ansalactam B (1) showed strong UV absorptions at 250, 290, and 315 nm, which indicated a highly conjugated aromatic compound. Infrared absorptions at 3402 and 1670  $cm^{-1}$  suggested the presence of hydroxyl and conjugated carbonyl groups, respectively. The  $^1H$  NMR spectrum of ansalactam B displayed a singlet aromatic proton H-8 ( $\delta_H$  7.79), three olefin protons H-13 ( $\delta_H$  6.39), H-15 ( $\delta_H$  5.41), H-17 ( $\delta_H$  4.77), one aromatic methyl singlet 7-

Received: March 28, 2016

Published: April 27, 2016

Me ( $\delta_{\text{H}}$  2.30), along with three methyl singlets 12-Me ( $\delta_{\text{H}}$  1.87), 14-Me ( $\delta_{\text{H}}$  1.69), 18-Me ( $\delta_{\text{H}}$  1.74) and four methyl doublets 16-Me ( $\delta_{\text{H}}$  1.09), 20-Me ( $\delta_{\text{H}}$  0.95), H-26 ( $\delta_{\text{H}}$  0.94), H-27 ( $\delta_{\text{H}}$  0.92) (see Table 1). The  $^{13}\text{C}$  NMR and 2D HSQC spectra indicated that eight methyl groups, one methylene, 10 methane carbons, and 14 quaternary carbons were present.

**Table 1. NMR Spectral Data for Ansalactam B (1)**  
(Methanol- $d_4$ )<sup>a</sup>

no.	$\delta_{\text{C}}$ , mult <sup>b</sup>	$\delta_{\text{H}}$ (mult, $J$ (Hz))	COSY	HMBC
1	196.8, qC			
2	72.7, qC			
3	69.7, CH	3.31		1, 2, 4, 10, 18, 19, 20, 21
4	195.6, qC			
5	128.0, qC			
6	167.8, qC			
7	136.4, qC			
8	131.5, CH	7.79, s		1, 6, 7, 9, 10
9	123.2, qC			
10	140.1, qC			
11	202.4, qC			
12	141.0, qC			
13	141.8, CH	6.39, s		11, 12-Me, 14-Me
14	134.7, qC			
15	135.9, CH	5.41, br s	16	13, 14, 14-Me, 16, 16-Me, 17
16	33.3, CH	2.97, m	15, 17	16-Me,
17	134.5, CH	4.77, d (8.0)	16	15, 6, 18-Me, 19
18	136.5, qC			
19	92.3, qC			
20	43.1, CH	2.47, qd (6.8, 4.3)	20-Me, 21	2, 19, 20-Me, 21, 22
21	59.2, CH	2.53, dd (9.0, 4.3)	20, 22	1, 2, 19, 20, 22, 23
22	43.4, CH	2.87, dt (9.0, 4.5)	21, 24	2, 20, 21, 23, 24, 25
23	183.8, qC			
24	45.4, CH <sub>2</sub>	1.61, m, 1.26, m	22, 25	21, 22, 23, 25, 26, 27
25	26.2, CH	1.78, m	24, 26, 27	22, 24, 26, 27
26	23.8, CH <sub>3</sub>	0.94, d (6.8)	25	24, 25, 27
27	22.5, CH <sub>3</sub>	0.92, d (6.8)	25	24, 25, 26
7-Me	17.5, CH <sub>3</sub>	2.30, s		6, 7, 8
12-Me	13.3, CH <sub>3</sub>	1.87, s		11, 12, 13
14-Me	23.3, CH <sub>3</sub>	1.69, s		13, 14, 15
16-Me	21.9, CH <sub>3</sub>	1.09, d (6.8)	16	15, 16, 17
18-Me	14.8, CH <sub>3</sub>	1.74, s		17, 18, 19
20-Me	11.0, CH <sub>3</sub>	0.95, d (6.8)	20	19, 20, 21

<sup>a</sup>600 MHz for  $^1\text{H}$  NMR and 75 MHz for  $^{13}\text{C}$  NMR. <sup>b</sup>Numbers of attached protons were determined by analysis of 2D spectra.

The planar structure of **1** was established from an analysis of 2D NMR spectroscopic data. Two spin systems consisting of eight carbon and four carbon units, respectively, were constructed from analysis of COSY correlations. The COSY crosspeaks [H-26, H-27/H-25/H24/H-22/H-21/H-20/20-Me] permitted the assignment of the eight-carbon side-chain fragment possessing a terminal *gem*-dimethyl group, while additional crosspeaks [H-15/H-16/H-17, H-16/16-Me] illus-

trated the second spin system with a four-carbon unit defining part of the polyene ring.

The dihydronaphthoquinone ring in **1** was established from the interpretation of heteronuclear multiple bond correlation (HMBC) spectroscopic data. The observation of long-range HMBC correlations from the aromatic singlet proton H-8 to four aromatic carbons C-6, C-7, C-9, C-10 and one ketone carbon C-1, from the aromatic methyl singlet 7-Me to the carbons C-6, C-7, and C-8, and from the methine proton H-3 to the carbons C-1, C-2, C-4, C-10 allowed the dihydronaphthoquinone ring system to be confidently assigned. Further, a two-bond HMBC correlation from H<sub>2</sub>-24 to carbon C-22 and a three-bond HMBC correlation from H<sub>2</sub>-24 to C-23 provided the attachment of a lactam carbonyl group at C-22. The chemical shifts of C-2 ( $\delta_{\text{C}}$  72.7), C-23 ( $\delta_{\text{C}}$  183.8), and the molecular formula of **1** suggested that they are connected through the nitrogen atom. A three-bond HMBC correlation from H-20 and H-22 to carbon C-2, and long-range HMBC correlations from H-3 to carbons C-4, C-18, C-19 ( $\delta_{\text{C}}$  92.3), C-20, and from H-21 to C-1, C-2, C-19, allowed the connection of C-21/C-2/C-3/C-19, illustrating the attachment of the tetracyclic ring system with a dihydro-naphthoquinone ring. The chemical shift of C-19 ( $\delta_{\text{C}}$  92.3) indicated the presence of a hydroxyl group at C-19.

Further, a long-range HMBC correlation from the methyl doublet 20-Me to the carbons C-19, C-20, and from the singlet methyl 18-Me to the carbons C-17, C-18, and C-19 permitted the attachment of C-18/C-19/C-20. The linkage between this unit and the second spin system possessing C-15, C-16, C-17, and 16-Me was established based on the long-range HMBC correlations from the methyl singlet 16-Me to the carbons C-15, C-16 and C-17. Long-range HMBC correlations from the methyl singlet 14-Me to C-13, C-14, C-15, and from the olefinic proton H-15 to carbons C-13, 14-Me, and from the methyl singlet 12-Me to carbons C-11, C-12, C-13 allowed the connectivity of C-11/C-12/C-13/C-14/C-15, completing the assignment of the side chain of the molecule. Lastly, the connection of C-11 to C-5 was derived from elimination of other possible carbon connections yielding the gross structure of **1** (Figure 1).

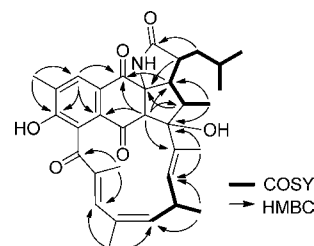


**Figure 1.** Key COSY and three-bond HMBC correlations allowing the planar structure of ansalactam B (**1**) to be assigned.

The 12*E*, 14*Z*, and 17*E* geometries of the trisubstituted double bonds were assigned on the basis of the chemical shifts of the attached methyl groups in the polyene ring. The chemical shift of 12-Me and 18-Me ( $\delta_{\text{C}}$  13.3 and  $\delta_{\text{C}}$  14.8) indicated 12*E*, 17*E* geometries, while the chemical shift of 14-Me ( $\delta_{\text{C}}$  23.3) suggested the *Z* configuration on this double bond.<sup>8</sup> The relative configurations of the tetracyclic six- and five-membered rings in **1** were assigned from analysis of ROESY NMR data. ROESY correlations (H-24/H-21/H-3/18-Me, H-21/H-20/H-17) indicated that H-3, H-20, H-21, and H-

24 are on the same face on the tetracyclic ring system. A ROESY correlation between H-22 and 20-Me also allowed these protons to be placed on the opposite site of the tetracyclic ring system. Energy-minimized modeling of **2** (Figure S21) and sharing the same biosynthetic origin with ansalactam A (**4**) revealed the  $R^*$  configurations of C-2 and the five-membered ring in **2** as shown in Figure 2.

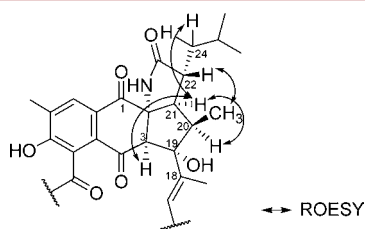


**Figure 2.** Key ROESY correlations used to establish the relative configuration of ansalactam B (**1**).

The molecular formula of ansalactam C (**2**) was assigned as  $C_{33}H_{41}NO_7$  on the basis of analysis of HRESIMS data (a protonated molecular ion at  $m/z$  564.2945  $[M + H]^+$ ). The  $^1H$  NMR spectrum of **2** was almost identical to that of **1** except for the presence of one more singlet aromatic proton H-5 ( $\delta_H$  6.88) and one methyl singlet 20-Me ( $\delta_H$  1.59) instead of a methyl doublet. The  $^{13}C$  NMR spectrum of **2** illustrated significant chemically shifted carbons [C-4 ( $\delta_C$  84.4), C-11 ( $\delta_C$  171.7), C-19 ( $\delta_C$  207.5), C-20 ( $\delta_C$  63.3)] compared to those of **1**. The presence of the aromatic singlet proton H-5, the chemical shift of the new carboxylic acid carbon, C-11, and the 18 amu addition of water to the molecular formula compared to **1** suggested that the carbon bond between C-5 and C-11 in **2** had been cleaved to yield the carboxylic acid functionality at C-11. The interpretation of long-range HMBC correlations allowed the planar structure of **2** to be assigned. Specifically, HMBC correlations from the singlet 20-Me to carbons C-4, C-19, C-20, and C-21 and from the methylene protons H-3 to carbons C-1, C-2, C-4, C-10, C-20, and C-21 permitted a bicyclo[3.2.1]octane ring configuration to be assigned in the molecule. The carbon chemical shift of C-4 ( $\delta_C$  84.4) also supported the hydroxy group at this position (Figure S1).

As in **1**, the geometries of the trisubstituted double bonds of **2** were assigned as 12*E*, 14*Z*, 17*E*, respectively, on the basis of the chemical shifts of the methyl groups. The relative configurations of the bicyclo[3.2.1]octane ring system in **2** were also established by analysis of ROESY correlations. ROESY correlations between 20-Me and H-22, between 20-Me and H-3, and between H-21 and H-24 indicated that H-3 methylene protons, the 20-Me, and H-22 should be placed on the same face of the bicyclic ring system, whereas H-21 and H-4 were placed on the opposite face as shown in Figure S2a.

The molecular formula of ansalactam D (**3**) was assigned as  $C_{33}H_{39}NO_6$  by interpretation of a protonated molecular ion peak at  $m/z$  546.2852  $[M + H]^+$  in the HRESIMS spectrum. The  $^1H$  NMR spectrum of **3** was almost identical to that of ansalactam A (**4**), a previously reported secondary metabolite from the same strain, except that **3** displayed two olefin protons H-15 ( $\delta_H$  5.77), H-17 ( $\delta_H$  6.24), and a methine proton H-13 ( $\delta_H$  5.77) instead of three olefin protons compared to those of **4**. The  $^1H$  NMR spectrum of **3** also displayed the singlet aromatic proton H-8 ( $\delta_H$  7.88), one aromatic methyl singlet 7-Me ( $\delta_H$  2.33) along with three methyl singlets 12-Me ( $\delta_H$

1.57), 14-Me ( $\delta_H$  2.38), and 18-Me ( $\delta_H$  0.79), and four methyl doublets 16-Me ( $\delta_H$  1.16), 20-Me ( $\delta_H$  1.07), H-26 ( $\delta_H$  1.05), and H-27 ( $\delta_H$  1.15). The  $^{13}C$  NMR spectrum of **3** showed 33 carbons including the two oxygenated carbons C-4 ( $\delta_C$  82.1), C-12 ( $\delta_C$  88.1), and one downfield-shifted methine carbon C-13 ( $\delta_C$  68.6). Long-range HMBC correlations from the methine proton H-13 to carbons C-3, C-4, C-10, C-11, C-12, 12-Me, C-14, C-15, from the methyl singlet 12-Me to carbons C-11, C-12, C-13, and from the methylene protons H-3 to carbons C-2, C-3, C-4, C-10 permitted the construction of a six-membered ring in the molecule. The chemical shift of C-4 ( $\delta_C$  82.1) and C-12 ( $\delta_C$  88.1), and considering the additional unsaturation in the molecular formula of **3**, allowed the ether linkage between C-4 and C-12 to be constructed. Further interpretation of 2D NMR spectroscopic data allowed the planar structure of **3** to be assigned as shown.

The relative configuration of **3** was assigned identical to that of ansalactam A (**4**) on the basis of the same biosynthetic origin. The small  $^1H$ – $^1H$  coupling constant between H-20 and H-21 (2.0 Hz) and ROESY correlations between H-21 and H-3 and between H-21 and H-24 also suggested that the relative configurations of C-2, C-20, C-21, and C-22 of **3** would be the same as those of **4** (Figure S2b). The ROESY correlations between 14-Me and H-15 and between H-15 and H-17 allowed the establishment of 14*Z* and 17*E* geometries, respectively. The relative configurations of the bicyclic ring system were assigned from analysis of ROESY correlations. ROESY correlations between 12-Me and H-13 and between 12-Me and 14-Me indicated that 12-Me and H-13 have a *syn* relationship. The ether linkage between C-4 and C-12 required that the cyclohexanone ring adopt a boat configuration. A ROESY correlation between 12-Me and H-13 indicated that these protons were in equatorial positions (Figure S22). An additional ROESY correlation between H-13 and H-20 also suggested that C-13/C-14 and C-20/C-21 bonds were located at the same face of the reduced quinone ring. These data allowed the relative configurations of C-4, C-12, and C-13 to be assigned as 4*R*\*, 12*S*\*, and 13*R*\*.

Ansamycin antibiotics generally consist of an aromatic moiety derived from the starter unit 3-amino-5-hydroxybenzoic acid (AHBA) coupled to an olefinic polyketide bridge (Figure 3).<sup>4</sup> The reported ansamycins can be distinguished by the assembling of two types of aromatic rings: a naphthalenic or naphthoquinone ring system for rifamycins, streptovaricins, and naphthomycins and a benzene or benzoquinone ring system found in ansamitocins and geldamycins. Biosynthetically, all ansamycins are assembled by a type I modular polyketide synthase (PKS).

Ansalactams A and D have a novel spiro- $\gamma$ -lactam ring connected with the dihydronaphthoquinone at C-2. Several  $\gamma/\epsilon$ -lactam-containing ansamycins have been also reported; an  $\epsilon$ -lactam ring in hygrocins B<sup>7</sup> and divergolide C<sup>9</sup> shared C-2/3 within the quinone ring, while the  $\gamma$ -lactam ring in hygrocins C–F,<sup>10</sup> produced by the genetically engineered *Streptomyces* sp., shared C-3/4 within the quinone ring. A simultaneous mutasynthesis has yielded the natural product C17BAs with an unnatural  $\gamma$ -lactam macrolide.<sup>11</sup> These differences of the lactam ring position in the molecules imply the presence of many different biosynthetic routes for  $\gamma/\epsilon$ -lactam ansamycins. Consequently, the spiro  $\gamma$ -lactam ring in these ansalactams is not usual. Interestingly, a recent study has revealed that activation of dormant ansamycin biosynthetic gene cluster



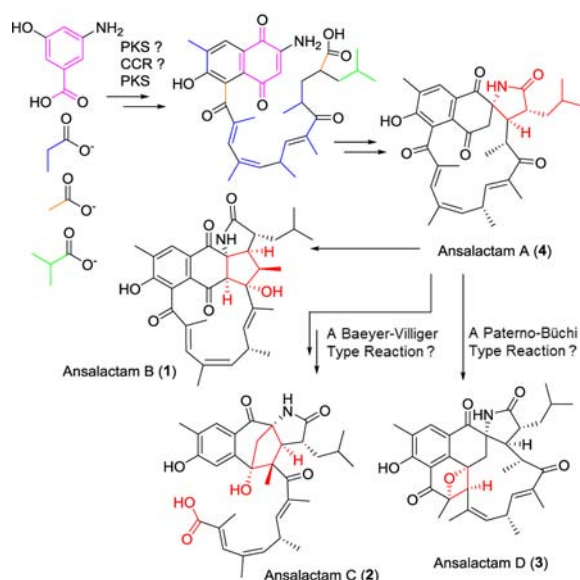


Figure 3. Proposed biosynthetic pathway for ansalactams A–D.

produced neoansamycin B and C with the same spiro  $\gamma$ -lactam ring system present.<sup>12</sup>

Ansalactams B–D (1–3) are new skeletal types illustrating atypical modifications in polyketide biosynthesis. Ansalactam C (2), which possesses the open polyketide chain, may be a product of a Baeyer–Villiger-style oxidation of the C-5 to C-11 bond. In addition, this metabolite also incorporates an unusual C-20 to C-4 ring contraction. Baeyer–Villiger monooxygenases (BVMOs) were found mostly in bacteria.<sup>13</sup> However, substrates for these known BVMOs are cyclic ketones or alkanes which do not include the aromatic ketone structure shown in ansalactam C. Ansalactam D (3) is most closely related to A (4), however, the additional oxetane ring appears, on structural grounds, to result from a formal 2 + 2 cycloaddition of the C-12–C-13 olefin to the C-4 ketone (Figure 3). This Paterno–Büchi-type reaction in organic synthesis is usually carried out with high energy illumination and an inorganic catalyst such as  $\text{Al}_2\text{O}_3$ . There is no reported enzyme that can catalyze this 2 + 2 cycloaddition biosynthetically.

Ansamycins display diverse bioactivities such as cell growth inhibition<sup>9</sup> and antibacterial<sup>5</sup> and Hsp90 inhibition activities.<sup>14</sup> Ansalactams A–D were not appreciably cytotoxic toward the HCT-116 colon carcinoma cell line and did not display inducible nitric oxide or acetylcholinesterase inhibition activities. Ansalactams B, C, and D were found to have a weak antibacterial activity against methicillin-resistant *S. aureus* (MRSA) with minimum inhibitory concentration (MIC) values of 31.2, 31.2, and 62.5  $\mu\text{g/mL}$ , respectively, while ansalactam A was inactive up to 100  $\mu\text{g/mL}$ .

## ■ ASSOCIATED CONTENT

### Supporting Information

The Supporting Information is available free of charge on the ACS Publications website at DOI: 10.1021/acs.orglett.6b00892.

Details of the collection and phylogenetic analysis of strain CNH-189, cultivation and extraction of strain CNH-189, isolation of 1–3, antibacterial assay, as well as complete NMR spectral data of 1–3 (PDF)

## ■ AUTHOR INFORMATION

### Corresponding Authors

\*E-mail: sjnam@ewha.ac.kr.

\*E-mail: wfenical@ucsd.edu.

### Author Contributions

<sup>§</sup>T.C.L. and I.Y. contributed equally.

### Notes

The authors declare no competing financial interest.

## ■ ACKNOWLEDGMENTS

The present study was supported by the Basic Science Research Program through the National Research Foundation of Korea (NRF), funded by the Ministry of Science, ICT & Future Planning (NRF-2014R1A1A1003492 and NRF-2016R1A2A1A05005078), and by the U.S. National Cancer Institute (NIH) under Grant No. R37CA044848 and Instrument Grant No. 1 S10 OD0106400-01A1 (HR–LC–MS, both to W.F.).

## ■ REFERENCES

- (1) Floss, H. G. *J. Nat. Prod.* **2006**, 69, 158–169.
- (2) Floss, H. G. *Nat. Prod. Rep.* **1997**, 14, 433–452.
- (3) Bérdy, J. *J. Antibiot.* **2005**, 58, 1–26.
- (4) (a) Fenical, W.; Jensen, P. R. *Nat. Chem. Biol.* **2006**, 2, 666–673. and references cited therein (b) Lam, K. S. *Curr. Opin. Microbiol.* **2006**, 9, 245–251.
- (5) (a) Jensen, P. R.; Gontang, E. A.; Mafnas, C.; Mincer, T. J.; Fenical, W. *Environ. Microbiol.* **2005**, 7, 1039–1048. (b) Gontang, E. A.; Fenical, W.; Jensen, P. R. *Appl. Environ. Microbiol.* **2007**, 73, 3272–3282.
- (6) Wilson, M. C.; Nam, S.-J.; Gulder, T. A. M.; Kauffman, C. A.; Jensen, P. R.; Fenical, W.; Moore, B. S. *J. Am. Chem. Soc.* **2011**, 133, 1971–1977.
- (7) Kaysser, L.; Bernhardt, P.; Nam, S.-J.; Loesgen, S.; Ruby, J. G.; Skewes-Cox, P.; Jensen, P. R.; Fenical, W.; Moore, B. S. *J. Am. Chem. Soc.* **2012**, 134, 11988–11991.
- (8) Maxwell, A.; Rampersad, D. *J. Nat. Prod.* **1989**, 52, 614–618.
- (9) Ding, L.; Maier, A.; Fiebig, H.-H.; Görls, H.; Lin, W.-H.; Peschel, G.; Hertweck, C. *Angew. Chem., Int. Ed.* **2011**, 50, 1630–1634.
- (10) Lu, C.; Li, Y.; Deng, J.; Li, S.; Shen, Y.; Wang, H.; Shen, Y. *J. Nat. Prod.* **2013**, 76, 2175–2179.
- (11) Song, Y. N.; Jiao, R. H.; Zhang, W. J.; Zhao, G. Y.; Dou, H.; Jiang, R.; Zhang, A. H.; Hou, Y. Y.; Bi, S. F.; Ge, H. M.; Tan, R. X. *Org. Lett.* **2015**, 17, 556–559.
- (12) Li, S.; Li, Y.; Lu, C.; Zhang, J.; Zhu, J.; Wang, H.; Shen, Y. *Org. Lett.* **2015**, 17, 3706–3709.
- (13) Whitesell, L.; Mimnaugh, E. G.; De Costa, B.; Myers, C. E.; Neckers, L. M. *Proc. Natl. Acad. Sci. U. S. A.* **1994**, 91, 8324–8328.
- (14) (a) Turfitt, G. E. *Biochem. J.* **1948**, 42, 376–383. (b) Fried, J.; Thoma, R. W.; Klingsberg, A. *J. Am. Chem. Soc.* **1953**, 75, 5764–5765. (c) Urbanczyk, J. M.; Soloduchko, J.; Zabza, A.; Sodano, G.; Grassi, A. *J. Basic Microbiol.* **1993**, 33, 141–146. (d) Wright, J. L. C.; Hu, T.; McLachlan, J. L.; Needham, J.; Walter, J. A. *J. Am. Chem. Soc.* **1996**, 118, 8757–8758.